

Hyperfine structures and the field effects of IBr molecule in its rovibronic ground state

Defu Wang(王得富), Xuping Shao(邵旭萍), Yunxia Huang(黄云霞), Chuanliang Li(李传亮), and Xiaohua Yang(杨晓华)

Citation: Chin. Phys. B, 2021, 30 (**11**): 113301. DOI: 10.1088/1674-1056/abfc3d
Journal homepage: http://cpb.iphy.ac.cn; http://iopscience.iop.org/cpb

What follows is a list of articles you may be interested in

---

^{57}Fe Mössbauer spectrometry: A powerful technique to analyze the magnetic and phase characteristics in RE-Fe-B permanent magnets

Lizhong Zhao(赵利忠), Xuefeng Zhang(张雪峰), Mi Yan(严密), Zhongwu Liu(刘仲武), and Jean-Marc Greneche
Chin. Phys. B, 2021, 30 (**1**): 013302. DOI: 10.1088/1674-1056/abc53d

Stark effect of the hyperfine structure of ICl in its rovibronic ground state: Towards further molecular cooling

Qing-Hui Wang(王庆辉), Xu-Ping Shao(邵旭萍), Xiao-Hua Yang(杨晓华)
Chin. Phys. B, 2016, 25 (**1**): 013301. DOI: 10.1088/1674-1056/25/1/013301

High-resolution photoassociation spectroscopy of ultracold Cs_2 long-range 0_g^- state： The external well potential depth

Liu Wen-Liang, Wu Ji-Zhou, Ma Jie, Xiao Lian-Tuan, Jia Suo-Tang
Chin. Phys. B, 2014, 23 (**1**): 013301. DOI: 10.1088/1674-1056/23/1/013301

High resolution photoassociation spectra of an ultracold Cs_2 long-range 0_u^+ ($6S_{1/2}$+$6P_{1/2}$) state

Chen Peng, Li Yu-Qing, Zhang Yi-Chi, Wu Ji-Zhou, Ma Jie, Xiao Lian-Tuan, Jia Suo-Tang
Chin. Phys. B, 2013, 22 (**9**): 093301. DOI: 10.1088/1674-1056/22/9/093301

Reanalysis of the photoassociation spectrum of $^{133}Cs_2$ ($6P_{3/2}$) 1_g state

Ma Jie, Li Yu-Qing, Wu Ji-Zhou, Fan Qun-Chao, Feng Hao, Sun Wei-Guo, Xiao Lian-Tuan, Jia Suo-Tang
Chin. Phys. B, 2013, 22 (**8**): 083302. DOI: 10.1088/1674-1056/22/8/083302

Hyperfine structures and the field effects of IBr molecule in its rovibronic ground state*

Defu Wang(王得富)[1], Xuping Shao(邵旭萍)[1], Yunxia Huang(黄云霞)[1], Chuanliang Li(李传亮)[2], and Xiaohua Yang(杨晓华)[1,†]

[1] School of Science, Nantong University, Nantong 226019, China
[2] Department of Physics, Taiyuan University of Science and Technology, Taiyuan 03324, China

(Received 14 January 2021; revised manuscript received 2 April 2021; accepted manuscript online 28 April 2021)

Hyperfine structures and the field effects of IBr molecule in its rovibronic ground state are theoretically studied by diagonalizing the effective Hamiltonian matrix. Perturbations of high-J levels up to 4 are taken into account when studying the hyperfine sub-levels of the $J = 0$ level, and thus, an 80×80 matrix is constructed and solved. Some of the experimentally absent molecular constants are computed using Dalton program. Our results will be helpful in the experimental investigation of manipulation and further cooling of cold IBr molecules.

Keywords: hyperfine structure, Zeeman effect, Stark effect, IBr molecule

PACS: 33.15.Pw, 32.60.+i **DOI:** 10.1088/1674-1056/abfc3d

1. Introduction

Molecule hyperfine structure provides additional degrees of freedom to manipulate cold molecules and new opportunities for sensitive probe of fundamental physics, and the molecular hyperfine structures can be investigated via molecular spectroscopy. However, the hyperfine shifts and separations are so small that they are usually concealed in the Doppler broadening due to the random thermal motion of the molecules.

Owing to the development of the molecular cooling in the past two decades[1–5] and the development of the laser single mode techniques, the hyperfine structures of molecules can be observed in laboratory precisely at present. Also the Zeeman and Stark effects of the molecules at hyperfine levels can be studied experimentally. Thus, the deduced field effects of the molecules may help experimentalists to manipulate or even to further cool cold molecules by means of the external magnetic and/or electric fields.

Polar molecules, due to that their anisotropic and long-range dipolar interactions add new ingredients to strongly correlated and collective quantum dynamics in many-body systems, are of great importance in the field of cold molecular physics, and alkali molecules are achieved coldest molecules so far. Therefore, heteronuclear (polar) alkali diatomic molecules have attracted many attentions.[6–10] Degenerate Fermi KRb ultracold molecules, associated from laser-cooled atoms, were achieved in the group of Ye by using Feshbach resonance followed by stimulated Raman adiabatic passage.[6] However, alkali heteronuclear molecules suffer from their short lifetimes due to chemical reaction,[6] which will undoubtedly limit their applications in the field of cold molecular physics. By contrast, heteronuclear halogen diatomic molecules are chemically stable, and thus, their ultracold molecules most probably have wider applications.[11–13] Thus, the study of the hyperfine structures together with their Zeeman and Stark effects of halogen diatomic molecules are essential. It is worth noting that heteronuclear halogen diatomic molecules could be slowed by our proposed near-resonant-laser-assisted Stark deceleration scheme[14] to the equivalent temperature at the order of microkelvin.

In addition, the electronic ground state of Iodine monobromide (IBr) is of $^1\Sigma$ symmetry, so that its ground state has neither Zeeman nor Stark effect at rotational level. However, it has both Zeeman and Stark effects at hyperfine level. So it is a good candidate for studying field effect of the hyperfine levels as well.

2. Theory

2.1. Hyperfine structure

The Hamiltonian of the IBr concerning its hyperfine structure consists of electronic, vibrational, rotational, and hyperfine terms. When studying the vibronic ground state, the first two parts can be treated as a constant.

The well-known rotational term is

$$H_{\rm rot} = B_v J^2 - D_v J^2 J^2, \tag{1}$$

where B_v and D_v are the molecular rotational constant and its first order distortion, and J is the molecular total angular momentum excluding nuclear spins.

*Project supported by the National Natural Science Foundation of China (Grant Nos. 12004199, U1810129, 52076145, and 11904252).
†Corresponding author. E-mail: xhyang@ntu.edu.cn
© 2021 Chinese Physical Society and IOP Publishing Ltd

The hyperfine structures are caused by the interactions of nuclear spins with the molecular total angular momentum excluding the nuclear spins ($H_{\rm sr}$) and of the nuclear quadrupoles with the gradients of the electric field of the electrons surrounding at the nuclei ($H_{\rm Q}$). The two interactions can be written as

$$H_{\rm sr} = C_1 \boldsymbol{I}_1 \cdot \boldsymbol{J} + C_2 \boldsymbol{I}_2 \cdot \boldsymbol{J}, \tag{2}$$

$$H_{\rm Q} = e^2 T^{(2)}(Q) : T^{(2)}(\nabla E), \tag{3}$$

where I_i is the nuclear spin and $i = 1$ or 2 denotes iodine (I) or bromine (Br) atom, and C_i is the nuclear spin–molecular rotation coupling constant and is expressed in Eqs. (1)–(3) in Ref. [15], e is the charge of an electron, $T^{(2)}(x)$ is the second rank tensor, and Q and ∇E represent the nuclear electric quadrupole and the gradient of the electric field of the electrons surrounding at nuclei, respectively.

The second rank tensors of Q and ∇E are as follows:[16]

$$T^{(2)}(Q) = \sum_p R_p^2 C^2(\theta_p, \phi_p), \tag{4}$$

$$T^{(2)}(\nabla E) = -\frac{1}{4\pi\varepsilon_0} \sum_i \frac{e_i}{R_i^3} C^2(\theta_i, \phi_i), \tag{5}$$

where $\boldsymbol{R}_{\rm p}$ is the position of the p-th proton in the nucleus, e_i is the charge of the i-th electron ($-e$) with position $\boldsymbol{R}_i$ in the remainder of the molecule, and $C_q^{(l)}(\theta, \phi)$ are related to Legendre polynomial $\mathrm{P}_l(\cos\theta_{ip})$.

The coupling sequence of the momenta is, $F = I_2 + F_1 = I_2 + (J + I_1)$. That is, the spin of I first couples with J to form the intermediate momentum F_1 and then F_1 couples with the spin of Br to form the molecular total angular momentum F. Therefore, the Hamiltonian matrices of IBr can be deduced at the $|I_1 J F_1 I_2 F\rangle$ basis employing Wigner–Eckart theory as follows:[17–19]

$$\begin{aligned}
&\left\langle I_1 J' F_1' I_2 F' \right| H_{\rm rot} \left| I_1 J F_1 I_2 F \right\rangle \\
&= B_v J(J+1) - D_v J^2 (J+1)^2,
\end{aligned} \tag{6}$$

$$\begin{aligned}
&\left\langle I_1 J' F_1' I_2 F' \right| H_{\rm sr} \left| I_1 J F_1 I_2 F \right\rangle \\
&= (1/2) C_1 [F_1(F+1) - I_1(I_1+1) - J(J+1)],
\end{aligned} \tag{7}$$

$$\begin{aligned}
&\left\langle I_1 J' F_1' I_2 F' \right| H_{\rm Q(1)} \left| I_1 J F_1 I_2 F \right\rangle \\
&= (1/4) eQq_1 (-1)^{I_1 + 2J' + F_1'} [(2J+1)(2J'+1)]^{1/2} \\
&\quad \times \begin{Bmatrix} F_1' & J' & I_1 \\ 2 & I_1 & J \end{Bmatrix} \begin{pmatrix} J' & 2 & J \\ 0 & 0 & 0 \end{pmatrix} \begin{pmatrix} I_1 & 2 & I_1 \\ -I_1 & 0 & I_1 \end{pmatrix}^{-1},
\end{aligned} \tag{8}$$

$$\begin{aligned}
&\left\langle I_1 J' F_1' I_2 F' \right| H_{\rm Q(2)} \left| I_1 J F_1 I_2 F \right\rangle \\
&= (1/4) eQq_2 (-1)^{F_1 + I_2 + F + F_1' + J + J' + I_1} \\
&\quad \times [(2J+1)(2J'+1)(2F_1+1)(2F_1'+1)]^{1/2} \\
&\quad \times \begin{Bmatrix} F & I_2 & F_1' \\ 2 & F_1 & I_2 \end{Bmatrix} \begin{Bmatrix} I_1 & F_1' & J' \\ 2 & J & F_1 \end{Bmatrix} \\
&\quad \times \begin{pmatrix} J' & 2 & J \\ 0 & 0 & 0 \end{pmatrix} \begin{pmatrix} I_2 & 2 & I_2 \\ -I_2 & 0 & I_2 \end{pmatrix}^{-1},
\end{aligned} \tag{9}$$

with the selection rules of $J' = J$, $(J \pm 2)$ and $F_1' = F_1$, $(F_1 \pm 1)$, $(F_1 \pm 2)$. Here, eQq_i represents the nuclear electric quadrupole constant and C_2 is too small to be set at 0, and { } and ( ) are the Wigner 6-j and 3-j symbols, respectively.

2.2. Stark effect

Stark effect, due to the interaction of molecular electric dipole (μ) with an applied electric field (E_Z) at Z axis, of the hyperfine levels can be expressed as[16]

$$H_s = -T^{(1)}(\mu) : T^{(1)}(E_Z), \tag{10}$$

where $T^{(1)}(x)$ is the first rank tensor. The molecular total angular momentum F projects to Z axis to form projection quantum number M_F in weak field limit. Therefore, the Hamiltonian matrices at the basis of $|I_1 J F_1 I_2 F M_F\rangle$ can be written as[18]

$$\begin{aligned}
&\left\langle J' I_1 F_1' I_2 F' M_F' \right| H_s \left| J I_1 F_1 I_2 F M_F \right\rangle \\
&= \mu E_Z (-1)^{1+F+F'-M_F+2F_1'+J+J'+I_1+I_2} \\
&\quad \times [(2F+1)(2F'+1)(2J+1)(2J'+1)] \\
&\quad \times (2F_1+1)(2F_1'+1)^{1/2} \\
&\quad \times \begin{Bmatrix} I_2 & F & F_1 \\ 1 & F_1' & F' \end{Bmatrix} \begin{Bmatrix} I_1 & F_1 & J \\ 1 & J' & F_1' \end{Bmatrix} \\
&\quad \times \begin{pmatrix} J' & 1 & J \\ 0 & 0 & 0 \end{pmatrix} \begin{pmatrix} F' & 1 & F \\ -M_F & 0 & M_F \end{pmatrix},
\end{aligned} \tag{11}$$

with the selection rules of $J' = J \pm 1$; $F_1' = F_1$, $(F_1 \pm 1)$ and $F' = F, (F \pm 1)$.

2.3. Zeeman effect

Zeeman effect, due to the interaction of the molecular total angular momentum excluding nuclear spin and nuclear spins with an applied magnetic field (B_Z) at z axis, of the hyperfine levels can be expressed as[16]

$$H_z = -g_{\rm r} \mu_{\rm N} \boldsymbol{J} \cdot \boldsymbol{B} - \sum_{i=1}^{2} g_i \mu_{\rm N} \boldsymbol{I}_i \cdot \boldsymbol{B}(1 - \sigma_i), \tag{12}$$

where $g_{\rm r}$ is the molecular rotational Landé g-factor, g_i is the nuclear g-factor, $\mu_{\rm N}$ is the nuclear magnetic dipole, and σ_i is the shielding coefficient of electrons surrounding to the nuclear spin. One can find the detailed expressions of $g_{\rm r}$ and σ_i as Eq. (1.36) in Ref. [20] and as Eqs. (4)–(6) in Ref. [15], respectively.

Similarly, the molecular total angular momentum F projects to Z axis to form projection quantum number M_F in weak field limit. Thus, the Hamiltonian matrices of the Zeeman effect can be written as[17]

$$\begin{aligned}
&\left\langle J' I_1 F_1' I_2 F' M_F' \right| - g_{\rm r} \mu_{\rm N} J \cdot B \left| J I_1 F_1 I_2 F M_F \right\rangle \\
&= -\delta_{M_F, M_F'} g_{\rm r} \mu_{\rm N} B_Z (-1)^{F' - M_F' + 2F_1' + J + F + I_1 + I_2 + 1} \\
&\quad \times [(2F+1)(2F'+1)(2F_1+1)(2F_1'+1)]^{1/2} \\
&\quad \times [J(J+1)(2J+1)]^{1/2}
\end{aligned}$$

$$\times \begin{Bmatrix} J' & F_1' & I_1 \\ F_1 & J & 1 \end{Bmatrix} \begin{Bmatrix} F' & F_1' & I_2 \\ F_1 & F & 1 \end{Bmatrix} \begin{pmatrix} F' & 1 & F \\ -M_F' & 0 & M_F \end{pmatrix}, \quad (13)$$

$$\begin{aligned} &\langle J' I_1 F_1' I_2 F' M_F' | -g_1 \mu_N I_1 \cdot B(1-\sigma_1) | J I_1 F_1 I_2 F M_F \rangle \\ &= -\delta_{J,J'} \delta_{M_F,M_F'} g_1 \mu_N B_Z (1-\sigma_1) (-1)^{F'-M_F'+J'+F_1'+F+F_1+I_1+I_2} \\ &\times [(2F+1)(2F'+1)(2F_1+1)(2F_1'+1)]^{1/2} \\ &\times [I_1(I_1+1)(2I_1+1)]^{1/2} \\ &\times \begin{Bmatrix} I_1 & F_1' & J' \\ F_1 & I_1 & 1 \end{Bmatrix} \begin{Bmatrix} F_1' & F_1' & I_2 \\ F & F_1 & 1 \end{Bmatrix} \begin{pmatrix} F' & 1 & F \\ -M_F' & 0 & M_F' \end{pmatrix}, \end{aligned} \quad (14)$$

$$\begin{aligned} &\langle J' I_1 F_1' I_2 F' M_F' | -g_2 \mu_N I_2 \cdot B(1-\sigma_2) | J I_1 F_1 I_2 F M_F \rangle \\ &= -\delta_{M_F,M_F'} g_2 \mu_N B_Z (1-\sigma_2) (-1)^{F'-M_F'+F_1'+F'+I_2+1} \\ &\times [(2F+1)(2F'+1)(2F_1+1)]^{1/2} [I_2(I_2+1)(2I_2+1)]^{1/2} \\ &\times \begin{Bmatrix} I_2 & F & F_1' \\ F' & I_2 & 1 \end{Bmatrix} \begin{pmatrix} F' & 1 & F \\ -M_F' & 0 & M_F' \end{pmatrix}, \end{aligned} \quad (15)$$

where $\delta_{A,B}$ is the Kronecker delta, which represents the perturbation selection rules.

3. Results and discussion

3.1. Hyperfine structure

The molecular constants needed to compute the hyperfine structure of IBr in its vibronic ground state are listed in Table 1, and the nuclear spin–rotation coupling constant of I atom is calculated employing the Dalton program.[21] The spin of I and Br (both ^{79}Br and ^{81}Br) atoms are 5/2 and 3/2, respectively. Therefore, the hyperfine levels can be achieved by diagonalizing the Hamiltonian matrices of Eqs. (6)–(9), as plotted in Fig. 1. The quantum numbers and values (in unit MHz) of the levels are labeled as well. The assignment of the hyperfine levels is accomplished according to their eigenvectors. As evidenced in Fig. 1, the hyperfine structures of this two isotopologues only differ in value while the patterns appear almost the same. Thus, only the field effects of I^{79}Br will be stated in the following Subsection 3.2 and Subsection 3.3.

Table 1. Molecular constants (in units of MHz) of the vibronic ground state of IBr.

	I^{79}Br	I^{81}Br
B	1700.84269[b]	1674.97140[b]
D	0.0003057[b]	0.0002965[b]
eQq_{I}	−2753.50[a]	−2753.48[a]
eQq_{Br}	696.85[a]	582.05[a]
C_{I}	0.016[c]	0.014[c]

[a]Ref. [22], [b]Ref. [23], [c]calculated employing dalton.

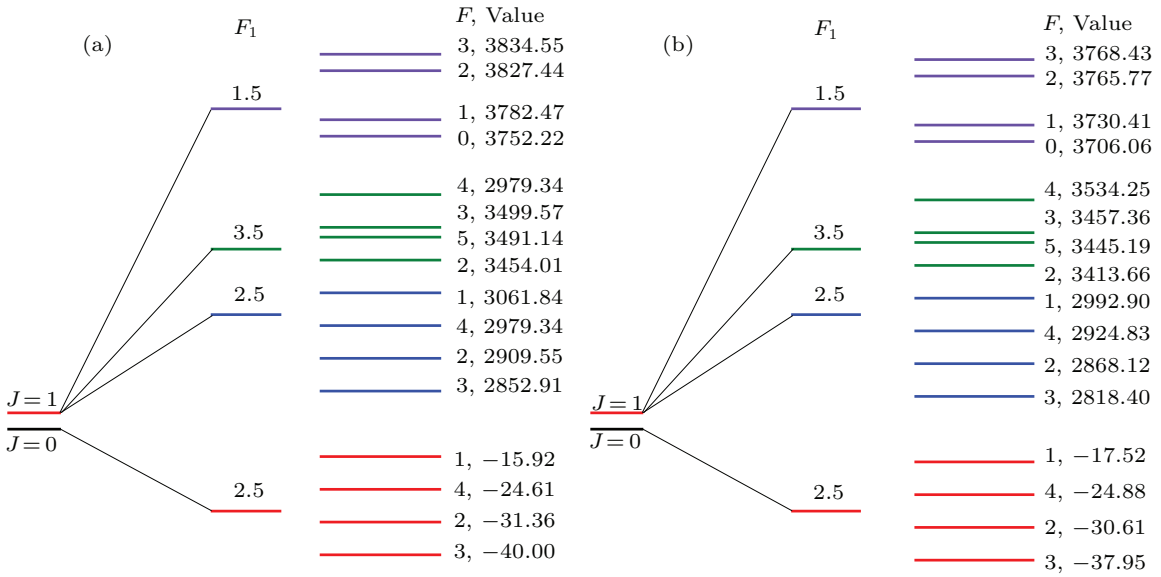


Fig. 1. Hyperfine levels (not scaled) of $J=0$ and 1 states in the rovibronic ground state of I^{79}Br (a) and I^{81}Br (b). The quantum numbers and the levels' values (in units of MHz) are labeled as well.

To verify our calculations, we try to predict the spectra to compare with the experimental values[22] as listed in Table 2. That the root-mean-squared error is 0.036 MHz, compared with the 83 experimental data,[22] *e.g.*, relative error of about 10^{-6}, suggests that our methods are correct.

As described in Eqs. (6)–(9), the rotationally perturbation selection rule to hyperfine levels is $\Delta J = 0, \pm 2$. Thus, the hyperfine levels of the $J=0$ state are directly perturbed by the $J=2$ state and indirectly perturbed by the $J=4$ and higher rotational states via intermediate states. Therefore, when studying the hyperfine levels of the rotational ground state, higher J states should be included in the Hamiltonian matrix. The hyperfine levels' relative corrections, defined as the perturbation correction over the value of the level, of the $J=0$ state due to the perturbation of the $J=4$ rotational state are listed in Table 3. Due to the little corrections of the $J=4$ state, the perturbations of higher rotational states are neglected and thus excluded in our Hamiltonian matrix. Therefore, the hyperfine levels are obtained by diagonalizing an 80×80 Hamiltonian matrix.

Table 2. Partial hyperfine spectra (in units of MHz) of the $J = 3 \leftarrow 2$ in the vobronic ground state of $I^{79}Br$.

F_1	F	Predicted	Experimental[22]	Error
9/2←9/2	5←5	9597.756	9597.848	0.092
9/2←9/2	4←5	9633.260	9633.324	0.064
9/2←9/2	4←4	9670.458	9670.518	0.060
9/2←9/2	3←3	9683.204	9683.265	0.061
3/2←1/2	2←2	9925.105	9925.124	0.019
3/2←1/2	2←1	9926.461	9926.481	0.020
3/2←1/2	1←2	9938.519	9938.538	0.019
3/2←1/2	1←1	9939.880	9939.894	0.014
5/2←3/2	3←3	9954.308	9954.314	0.006
5/2←3/2	1←1	9957.308	9957.312	0.004

Table 3. Relative corrections of the hyperfine levels when the perturbation of $J = 4$ state is included.

F	Relative correction
1	2.1×10^{-12}
2	-6.2×10^{-6}
3	2.9×10^{-6}
4	7.9×10^{-5}

3.2. Stark effect

In weak field limit, the total angular momentum $\boldsymbol{F}$ including nuclear spin projects to the applied electric field at Z axis to form projection quantum numbers M_F, where $M_F = 0, 1, \ldots, F$. Besides, the electric dipole of the $I^{79}Br$ of the rovibronic ground state is $\mu = 0.737$ Debye.[24] We find that the eigenvectors begin to show anomalous behavior when the applied field increasing more than 1000 V/cm, which implies that the angular momentum coupling sequence has become to change and our method does not work anymore. Figure 2 plots the Stark sublevels of the hyperfine levels varying with the applied electric field up to 1000 V/cm. Evidently, the $|J, F_1, F, M_F\rangle = |0, 2.5, 4, 4\rangle$ is perturbed downwards sharply at high electric field, and is found that it is perturbed by the $|1, 2.5, 4, 4\rangle$ level.

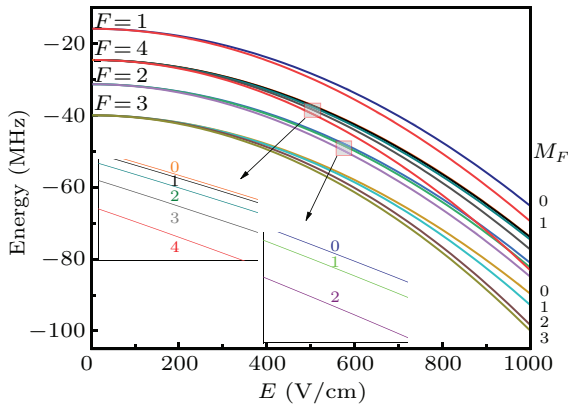


Fig. 2. Stark effects of the hyperfine levels of the rovibronic ground state ($J = 0$, $v = 0$, $X^1\Sigma$) of $I^{79}Br$ varying with the applied electric field. The quantum numbers of F and M_F are labeled as well.

3.3. Zeeman effect

Similar to that in the electric field, the total molecular angular momentum $\boldsymbol{F}$ projects to applied magnetic field to form M_F, where $M_F = -F, (-F+1), \ldots, 0, \ldots, (F-1), F$. Zeeman effect at the hyperfine levels comes from the interactions of the rotational magnetic moment and the nuclear spins to the applied magnetic field as expressed in Eq. (12). Nuclear magnetic dipole is $\mu_N = e\hbar/(2M_P)$, where $\hbar$ is reduced Planck constant, and M_P is the mass of a proton. Two g-factors and the shielding coefficients are absent experimentally, and thus are calculated with the Hatree–Fock method in the basis of Sadlej-pVTZ employing the Dalton program.[21] The calculation of nuclear shieldings using London Atomic Orbitals[25] to ensure fast basis set convergence and gauge origin independent results. The natural connection is used in order to get numerically accurate results. By default, the center of mass is chosen as gauge origin. The obtained parameters of $I^{79}Br$ are listed in Table 4, and those (both of ours and literature[26]) of $I^{35}Cl$ are also listed. The differences of the shielding coefficients are due to the latest vision program we used while those of the literature were obtained employing the previous vision. Nevertheless, we calculate the sublevels using two set of shielding coefficients and find that they only result in a relative error of about 10^{-4}.

Table 4. Molecular parameters needed in the studying of Zeeman effect at hyperfine level of $I^{79}Br$ and also those of $I^{35}Cl$ are listed for comparison.

	$I^{79}Br$	$I^{35}Cl$	
		This work	Ref. [26]
g_I	1.13	1.13	1.12
$g_{Br(Cl)}$	1.48	0.55	0.53
g_r	–0.01	–0.23	–0.36
σ_I (ppm)	2618	3521	4314
$\sigma_{Br(Cl)}$ (ppm)	3828	3330	1658
μ_N (J/T)	5.05×10^{-27}		

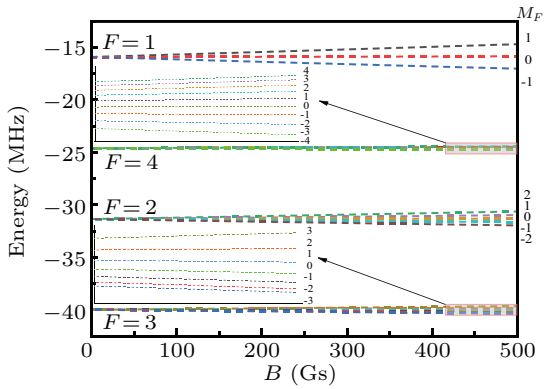


Fig. 3. Zeeman effects of the hyperfine levels of the rovibronic ground state ($J = 0$, $v = 0$, $X^1\Sigma$) of $I^{79}Br$ varying with the applied magnetic field. The quantum numbers of F and M_F are labeled as well.

Consequently, the Zeeman sublevels of the hyperfine levels can be achieved by diagonalizing the Hamiltonian matrices of Eqs. (13)–(15). Figure 3 plots the Zeeman sublevels varying with the applied magnetic field up to 500 Gs (1 Gs = 10^{-4} T). It shows that the splitting of the Zeeman sublevels decreases with the increasing of F. Unlike those of ICl,[26] the Zeeman sublevels with different M_F of $I^{79}Br$ does not cross each

other due to large hyperfine separations. Thus, the perturbations of the Zeeman sublevels do not apparently exhibit. However, when we get insight into the sublevels of the $F = 3$ level as shown in Fig. 4, we can also observe the slight perturbations of the sublevels due to their nonlinear responses to the applied field, even that the $|0, 2.5, 3, 3\rangle$ and $|0, 2.5, 3, -3\rangle$ levels are slightly perturbed by the $|0, 2.5, 4, 3\rangle$ and $|0, 2.5, 4, -3\rangle$ levels, respectively. The perturbation selection rules are summarized as: $\Delta J = 0, \pm 1$; $\Delta F_1 = 0, \pm 1$; $\Delta F = 0, \pm 1$; and $\Delta M_F = 0$.

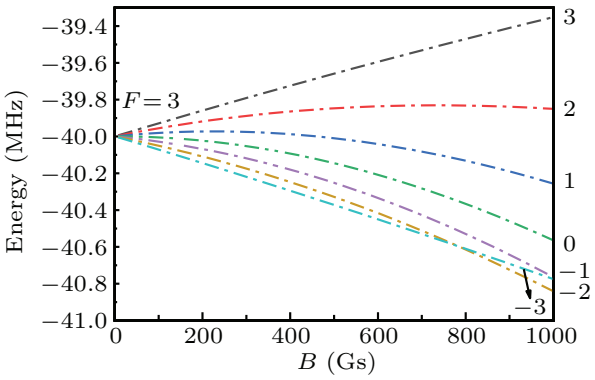


Fig. 4. Zeeman sub-levels of the $|J, F_1, F\rangle = |0, 2.5, 3\rangle$ level in the vobronic ground state of $I^{79}Br$ varying with the applied magnetic field.

4. Conclusion

Hyperfine structures of $I^{79}Br$ and $I^{81}Br$ in their rovibronic ground states are theoretically studied by diagonalizing the 80×80 effective Hamiltonian matrix, and our results are in good agreement with the experimental.[22] Thereafter, the Zeeman and Stark effects of the rovibrionic ground state of $I^{79}Br$ at hyperfine level are studied, perturbations of the sub-Zeeman and sub-Stark levels are observed. The results are essential in the field of manipulation and even further cooling of cold molecules via applying electric and/or magnetic fields.

References

[1] Aikawa K, Akamatsu D, Hayashi M, Oasa K, Kobayashi J, Naidon P, Kishimoto T, Ueda M and Inouye S 2010 *Phys. Rev. Lett.* **105** 203001
[2] Xu L, Yin Y, Wei B, Xia Y and Yin J 2016 *Phys. Rev. A* **93** 013408
[3] Ding S, Wu Y, Finneran I A, Burau J and Ye J 2020 *Phys. Rev. X* **10** 021049
[4] Bethlem H L, Berden G and Meijer G 1999 *Phys. Rev. Lett.* **83** 1558
[5] Hogan S D, Wiederkehr A W, Schmutz H and Merkt F 2008 *Phys. Rev. Lett.* **101** 143001
[6] Marco L D, Valtolina G, Matsuda K, Tobias W G, Covey J P and Ye J 2019 *Science* **363** 853
[7] Yang, H, Zhang D C, Liu L, Liu Y X, Nan J, Zhao B and Pan J W 2019 *Science* **363** 261
[8] Liu W L, Wu J Z, Ma J, Li P, Sovkov V B, Xiao L T and Jia S T 2016 *Phys. Rev. A* **94** 032518
[9] Blackmore J A, Sawant R, Gregory P D, *et al.* 2020 *Phys. Rev. A* **102** 053316
[10] Park J W, Will S A and Zwierlein M W 2015 *Phys. Rev. Lett.* **114** 205302
[11] Krems R V, Stwalley W C and Friedrich B 2009 *Cold Molecules: Theory, Experiment, Applications* (CRC Press)
[12] Rajapakse R M, Bragdon T, Rey A M, Calarco T and Yelin S F 2009 *Phys. Rev. A* **80** 013810
[13] Tarbutt M R, Hudson J J, Sauer B E and Hinds E A 2009 *Faraday Discuss.* **142** 37
[14] Gu Y F, Chen K, Huang Y X and Yang X H 2019 *Chin. Phys. B* **28** 043702
[15] Müller H S P and Gerry M C L 1995 *J. Chem. Phys.* **103** 577
[16] Brown J M and Carrington A 2003 *Rotational Spectroscopy of Diatomic Molecules* (Cambridge: Cambridge University Press)
[17] Carrington A, Howard B J, Levy D H and Robertson J C 1967 *Mol. Phys.* **15** 187
[18] Edmonds A R *Angular Momentum in Quantum Mechanics* (Princeton: Princeton University Press)
[19] Curl R F and Kinsey J L 1961 *J. Chem. Phys.* **35** 1758
[20] Ogilvie J F, Oddershede J and Sauer S P A 2000 *The Rotational g Factor of Diatomic Molecules in State* $1\Sigma^+$ *or* 0^+
[21] Aidas K, Angeli C, Bak K L, BaK K L, *et al.* 2014 *Wires. Comput. Mol. Sci.* **4** 269
[22] Tiemann E and Möller T 1975 *Z. Nat. A* **30** 986
[23] Campbell J M and Bernath P F 1993 *J. Mol. Spectrosc.* **158** 339
[24] Tiemann E and Dreyer 1977 *Chem. Phys.* **23** 231
[25] Hameka H F 1958 *Mol. Phys.* **1** 203
[26] Chen K, Hu Z, Wang Q H and Yang X H 2017 *Chin. Phys. Lett.* **34** 103302